Electronic Supplementary Information for

Synthesis and comparative studies of K-region functionalized pyrene derivatives

*Farshid Shahrokhi, Roxana Fazli Estabragh, and Yuming Zhao**

Department of Chemistry, Memorial University of Newfoundland
St. John's, NL, Canada A1B 3X7

Email: yuming@mun.ca

Table of Content

1. NMR Spectra for New Compounds

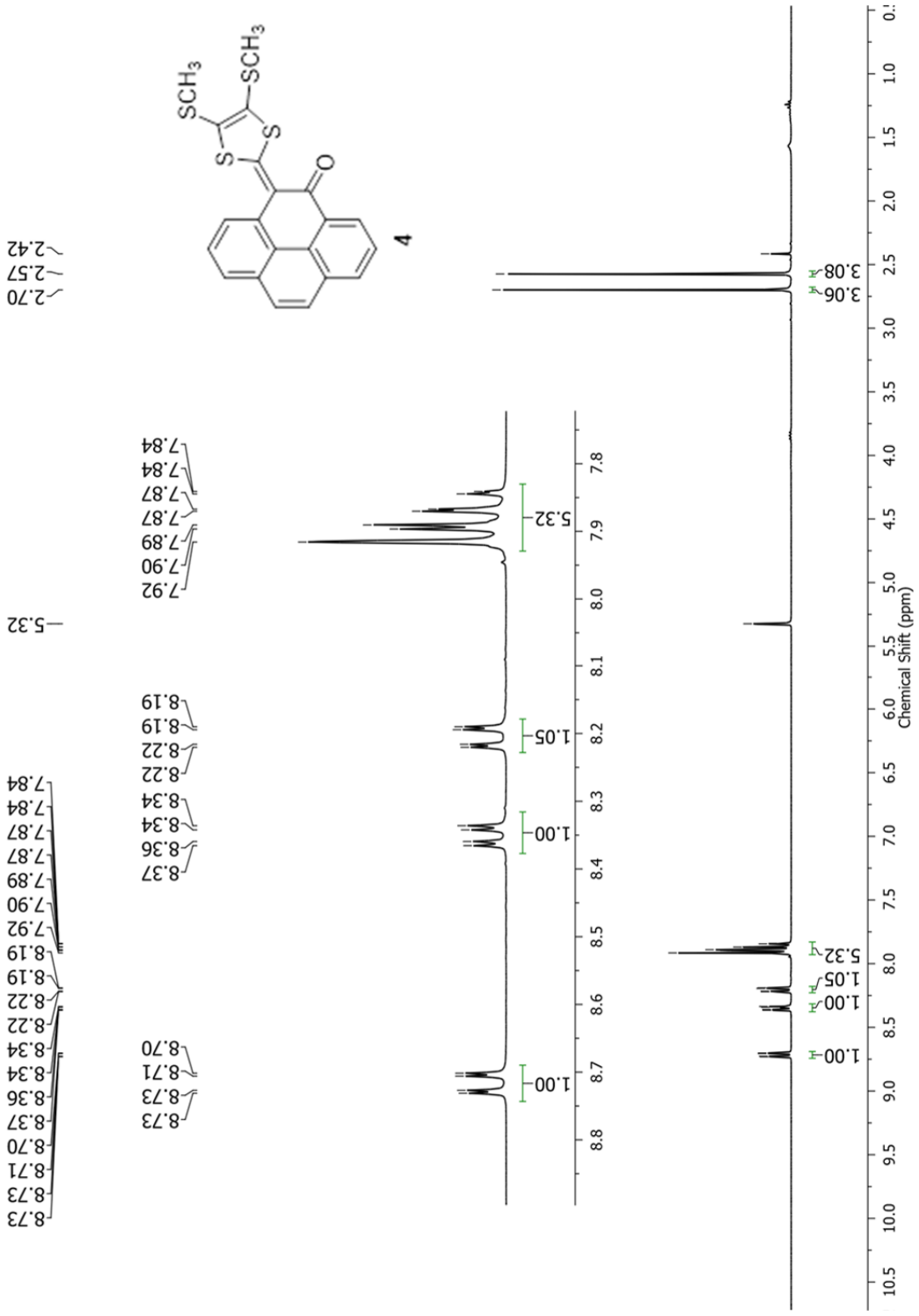

Fig. S-1 ^{1}H NMR (300 MHz, CD_2Cl_2) of compound **4**.

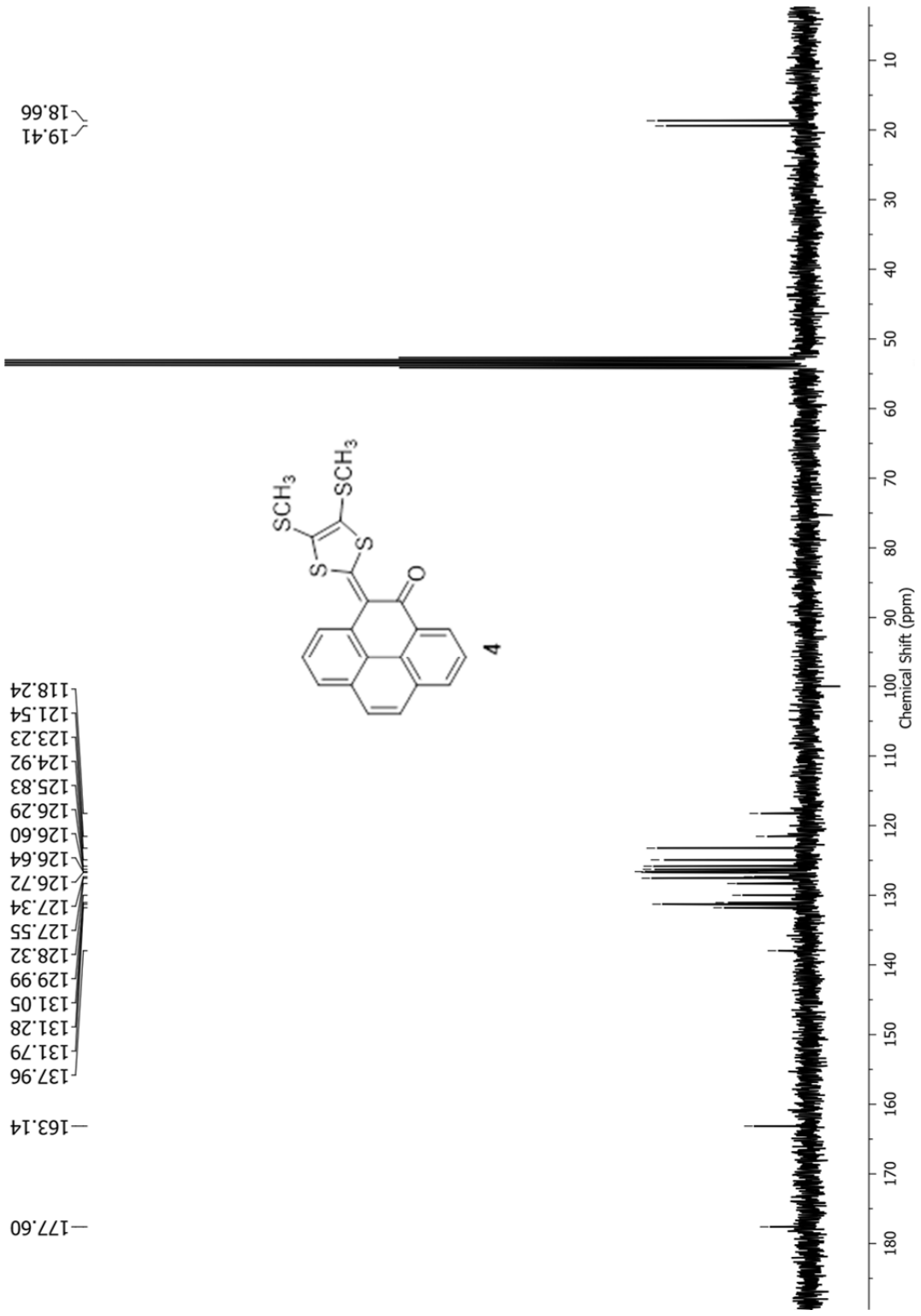

Fig. S-2 ^{13}C NMR (75 MHz, CD_2Cl_2) of compound **4**.

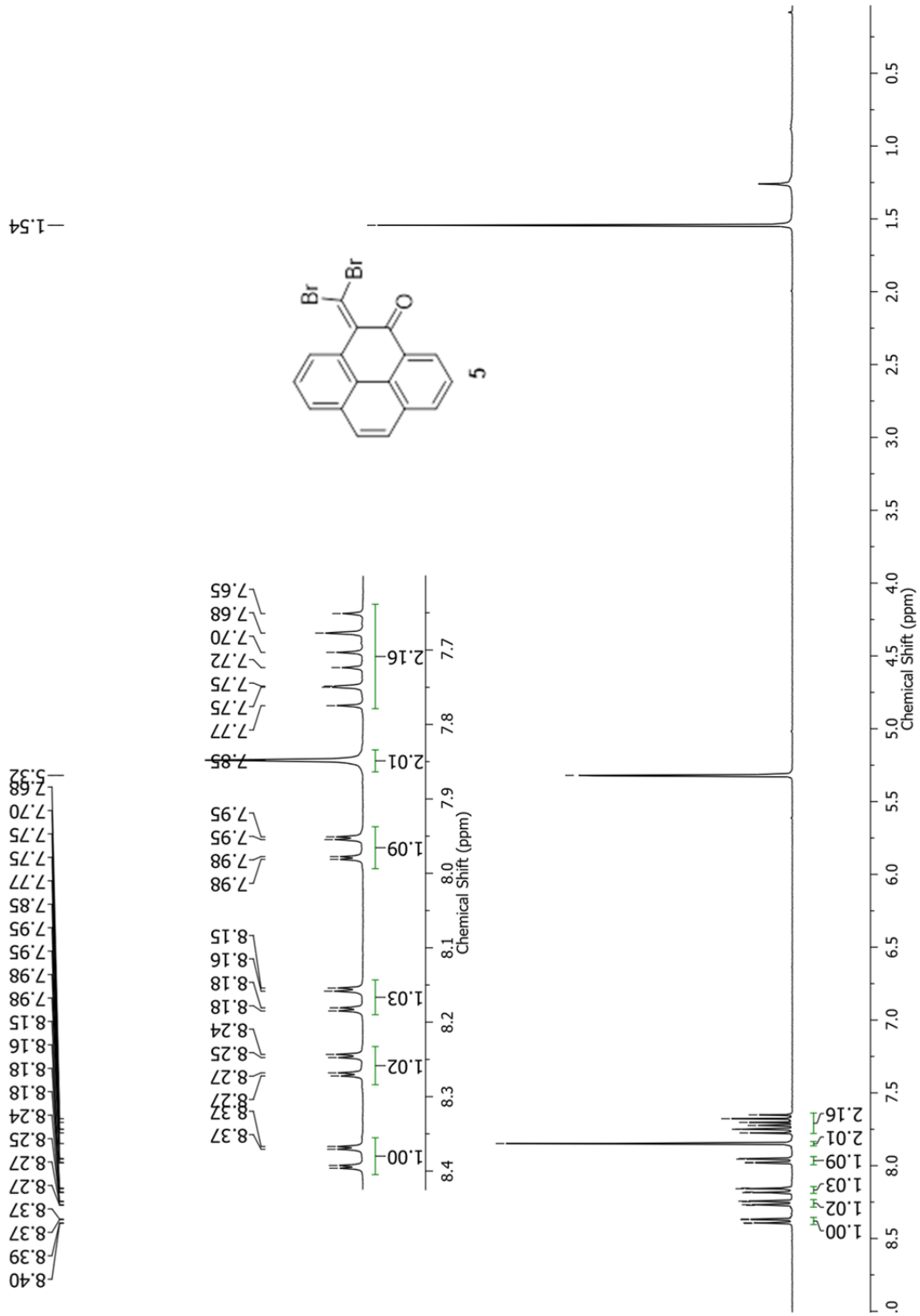

Fig. S-3 ^{1}H NMR (300 MHz, CD_2Cl_2) of compound **5**.

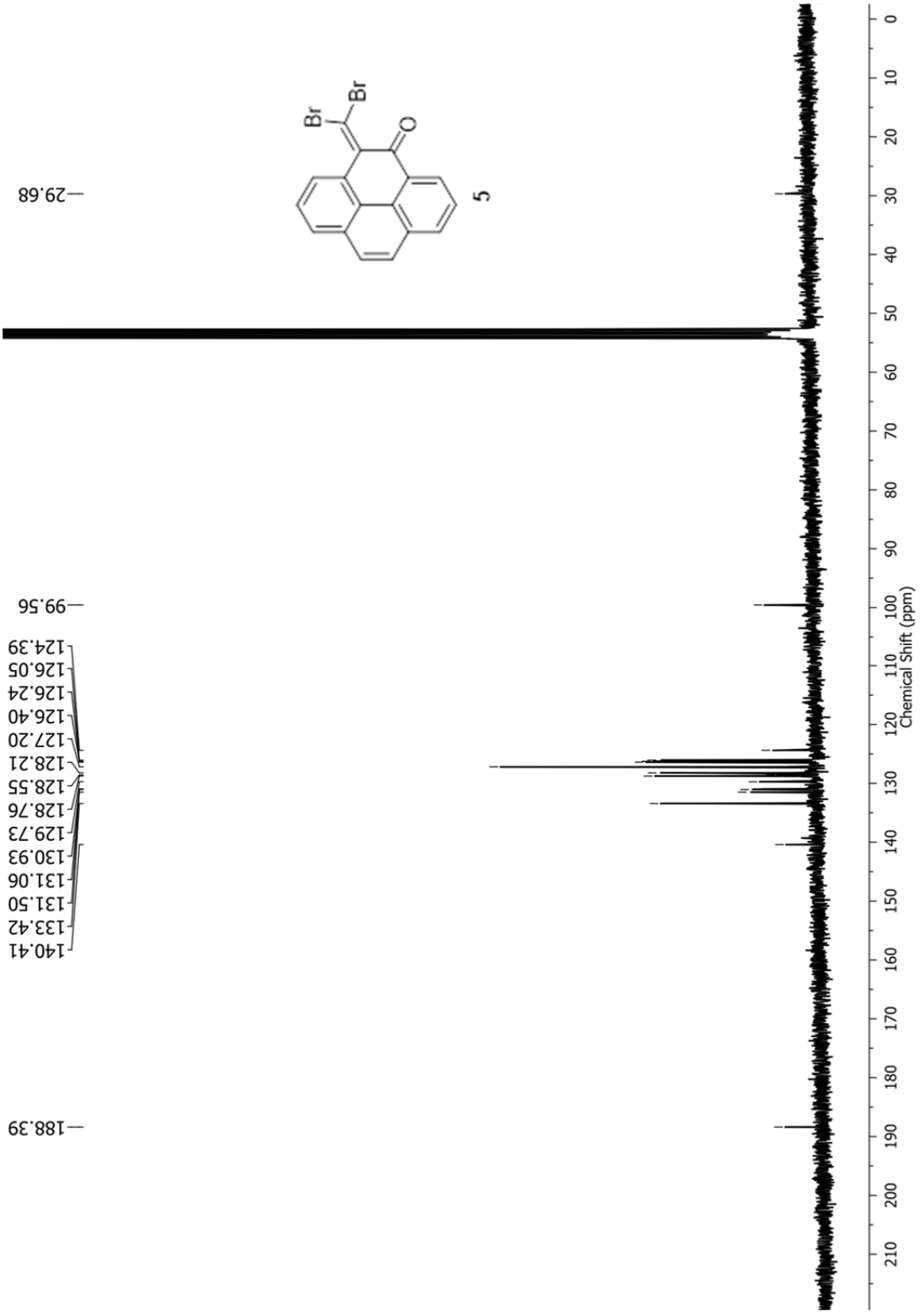

Fig. S-4 ^{13}C NMR (75 MHz, CD_2Cl_2) of compound **5**.

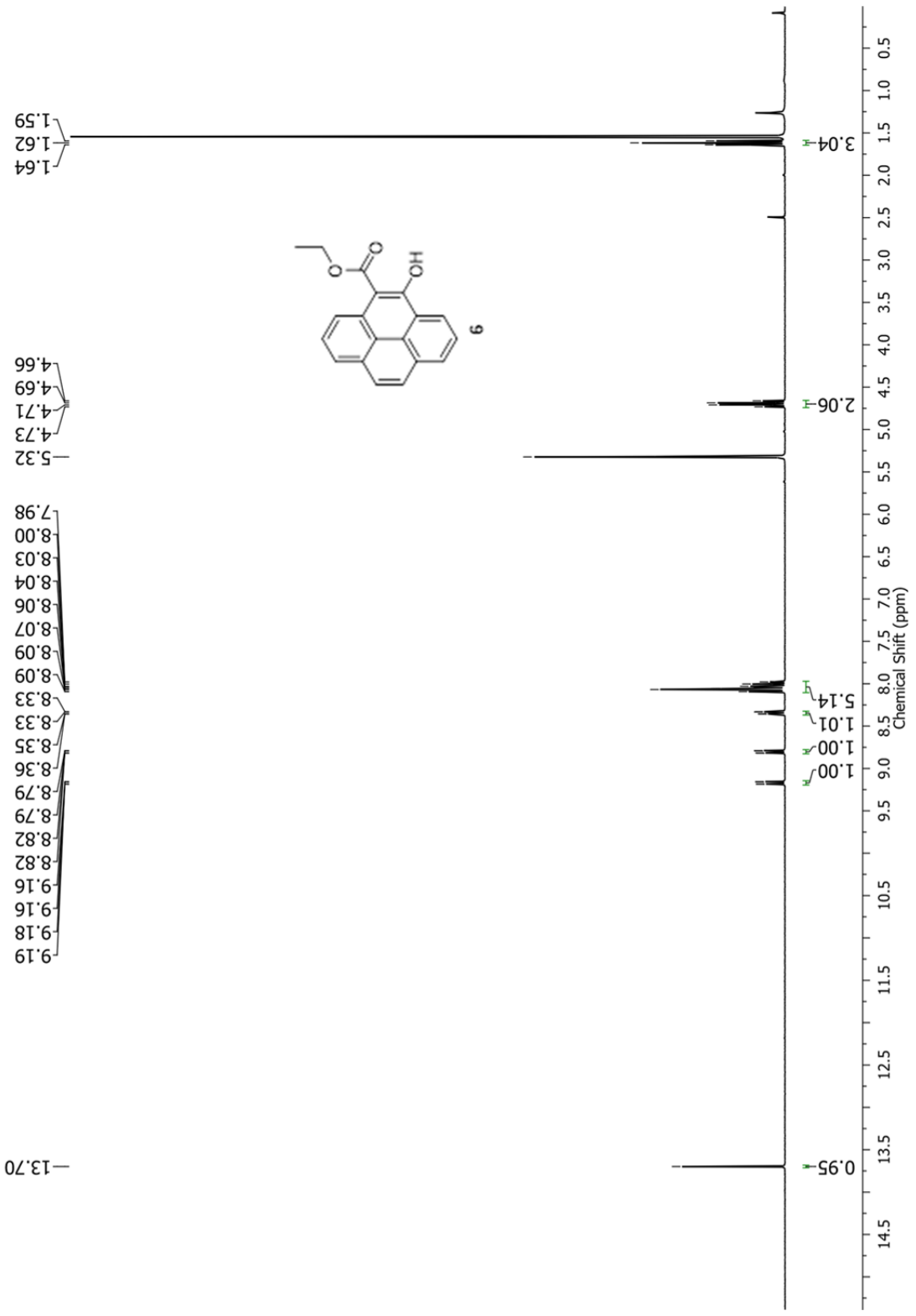

Fig. S-5 ^{1}H NMR (300 MHz, CD_2Cl_2) of compound **6**.

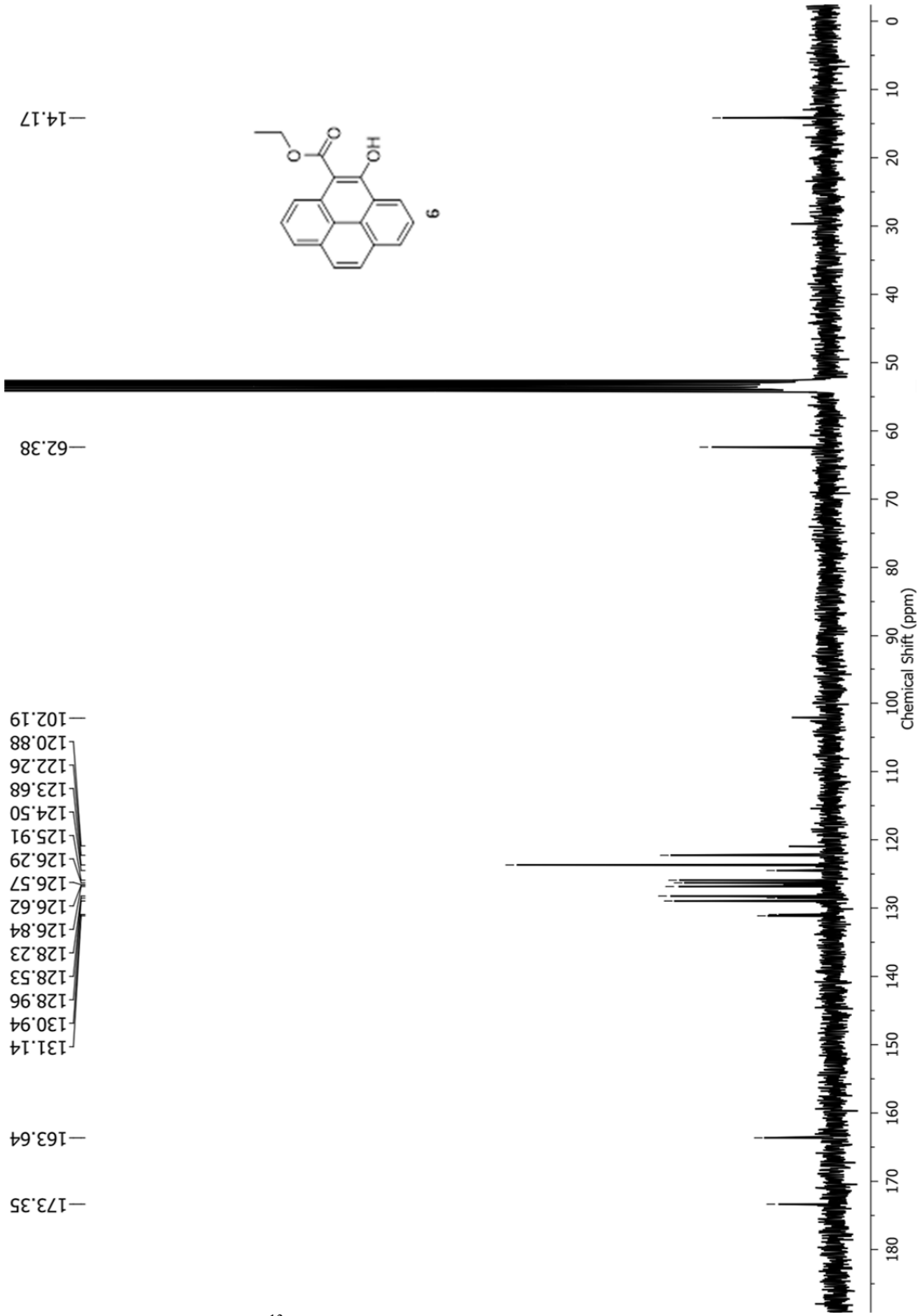

Fig. S-6 ^{13}C NMR (75 MHz, CD_2Cl_2) of compound **6**.

2. Optimization of the Synthesis of 4

Table S-1 Optimization of the synthetic conditions for compound **4**

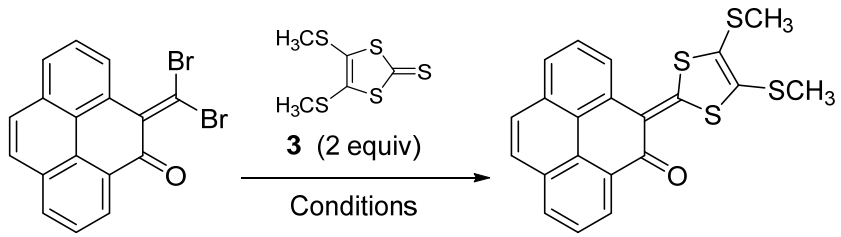

5 **4**

Entry	Solvent	Base	Temperature	Time	Yield
1	EtOH	KOH (10 eq)	80 °C	45 min	45%
2	EtOH	KOH (4 eq)	80 °C	45 min	45%
3	EtOH	KOH (2 eq)	80 °C	45 min	10%
4	EtOH	NH_4OH (4 eq)	80 °C	45 min	trace
5	EtOH	Pyridine (4 eq)	80 °C	45 min	0%
6	EtOH	Imidazole (4 eq)	80 °C	45 min	0
7	EtOH	Bu_4NOH	80 °C	45 min	35%
8	Dioxane	Bu_4NOH	80 °C	45 min	0%
9	THF/water	KOH (4 eq)	80 °C	45 min	0%
10	DMF	KOH (4 eq)	80 °C	45 min	0%
11	EtOH	KOH (4 eq)	rt	45 min	32%
12	EtOH	KOH (4 eq)	120 °C	45 min	40%
13	EtOH	KOH (4 eq)	80 °C	10 min	25%

3. Crystal Data and Refinement of 4-6

Table S-2 Crystal data and structure refinement of **4**

Empirical formula	$C_{21}H_{14}OS_4$
Formula weight	410.56
Temperature/K	100(2)
Crystal system	monoclinic
Space group	$P2_1/c$
a/Å	5.15876(6)
b/Å	20.4115(3)
c/Å	16.5822(2)
β/°	96.4856(12)
Volume/Å^3	1734.90(4)
Z	4
ρ_{calc}g/cm^3	1.572
μ/mm^{-1}	5.091
F(000)	848.0
Crystal size/mm^3	0.193 × 0.04 × 0.034
Radiation	Cu $K\alpha$ (λ = 1.54184)
2θ range for data collection/°	6.894 to 154.812
Index ranges	$-6 \le h \le 6$, $-25 \le k \le 25$, $-16 \le l \le 20$
Reflections collected	42353
Independent reflections	3667 [R_{int} = 0.0638, R_{sigma} = 0.0255]
Data/restraints/parameters	3667/0/237
Goodness-of-fit on F^2	1.032
Final R indexes [I>=2σ (I)]	R_1 = 0.0391, wR_2 = 0.1045
Final R indexes [all data]	R_1 = 0.0427, wR_2 = 0.1067
Largest diff. peak/hole / e Å^{-3}	0.61/-0.35

Table S-3 Crystal data and structure refinement of **5**

Empirical formula	$C_{17}H_8Br_2O$
Formula weight	388.05
Temperature/K	100(2)
Crystal system	monoclinic
Space group	$P2_1/c$
a/Å	3.88283(4)
b/Å	18.75250(17)
c/Å	17.4959(2)
β/°	92.4372(10)
Volume/Å^3	1272.77(2)
Z	4
ρ_{calc}g/cm^3	2.025
μ/mm^{-1}	7.994
F(000)	752.0
Crystal size/mm^3	0.12 × 0.06 × 0.05
Radiation	Cu $K\alpha$ (λ = 1.54184)
2θ range for data collection/°	6.914 to 154.478
Index ranges	$-4 \le h \le 4$, $-23 \le k \le 20$, $-22 \le l \le 21$
Reflections collected	16339
Independent reflections	2654 [R_{int} = 0.0565, R_{sigma} = 0.0330]
Data/restraints/parameters	2654/0/181
Goodness-of-fit on F^2	1.088
Final R indexes [I>=2σ (I)]	R_1 = 0.0277, wR_2 = 0.0720
Final R indexes [all data]	R_1 = 0.0303, wR_2 = 0.0736
Largest diff. peak/hole / e Å^{-3}	0.43/-0.56

Table S-4 Crystal data and structure refinement of **6**

Empirical formula	$C_{19}H_{14}O_3$
Formula weight	290.30
Temperature/K	100(2)
Crystal system	monoclinic
Space group	$P2_1/c$
a/Å	14.9879(7)
b/Å	4.96700(10)
c/Å	18.9991(7)
β/°	105.932(4)
Volume/Å^3	1360.06(9)
Z	4
ρ_{calc}g/cm^3	1.418
μ/mm^{-1}	0.773
F(000)	608.0
Crystal size/mm^3	0.2 × 0.1 × 0.05
Radiation	Cu $K\alpha$ (λ = 1.54184)
2θ range for data collection/°	6.132 to 154.814
Index ranges	$-18 \le h \le 18$, $-6 \le k \le 5$, $-24 \le l \le 23$
Reflections collected	17708
Independent reflections	2855 [R_{int} = 0.0450, R_{sigma} = 0.0302]
Data/restraints/parameters	2855/0/201
Goodness-of-fit on F^2	1.081
Final R indexes [I>=2σ (I)]	R_1 = 0.0641, wR_2 = 0.1896
Final R indexes [all data]	R_1 = 0.0710, wR_2 = 0.1968
Largest diff. peak/hole / e Å^{-3}	0.47/-0.25

4. Results of TD-DFT Calculations of 4-6

Table S-5 Summary of vertical electronic transition properties of **4** computed at the TD-CAM-B3LYP/6-311+G(d,p) level of theory

Wavelength (nm)	***f***	**MO Contributions**
416.2	0.5839	HOMO→LUMO (93%)
331.8	0.0047	H-5→LUMO (61%), H-1→LUMO (17%)
325.0	0.0355	H-5→LUMO (11%), H-1→LUMO (45%), HOMO→L+1 (17%)
316.5	0.0228	H-2→LUMO (66%)
295.8	0.2926	H-1→LUMO (26%), HOMO→L+1 (51%)
284.6	0.0921	H-2→LUMO (12%), H-2→L+1 (23%), H-1→L+2 (11%), HOMO→L+2 (22%)
277.1	0.0425	HOMO→L+4 (26%), HOMO→L+5 (38%)
269.6	0.0168	H-3→LUMO (22%), H-1→L+1 (35%)
265.9	0.1874	H-3→LUMO (18%), HOMOvL+3 (30%), HOMO→L+5 (10%)
262.1	0.1973	H-3→LUMO (18%), H-1→L+1 (14%), HOMO→L+2 (33%)
250.8	0.0426	HOMO→L+3 (16%), HOMO→L+4 (17%)
248.4	0.0501	H-4→LUMO (11%), H-2→L+1 (13%), HOMO→L+4 (12%)
245.9	0.0194	H-4→LUMO (13%), HOMO→L+4 (17%), HOMO→L+6 (15%), HOMO→L+9 (14%)
242.3	0.0645	H-4→LUMO (43%)
238.3	0.1028	H-6→LUMO (36%), H-2→L+2 (10%), HOMO→L+8 (17%)
230.3	0.3358	H-2→L+1 (16%), H-2→L+2 (20%), H-1→L+1 (10%), H-1→L+2 (31%)
228.0	0.0175	HOMO→L+6 (10%), HOMO→L+7 (26%)
225.2	0.1466	H-6→LUMO (33%), HOMO→L+8 (25%)
223.9	0.0107	HOMO→L+6 (10%), HOMO→L+10 (27%)
220.6	0.7142	H-3→L+2 (10%), H-2→L+2 (33%), H-1→L+2 (20%)

Table S-6 Summary of vertical electronic transition properties of **5** computed at the TD-CAM-B3LYP/6-311+G(d,p) level of theory

Wavelength (nm)	***f***	**MO Contributions**
367.0	0.1078	H-3→LUMO (15%), HOMO→LUMO (69%)
331.8	0.0565	H-3→LUMO (33%), H-1→LUMO (26%), HOMO→LUMO (23%)
326.4	0.0191	H-3→LUMO (21%), H-1→LUMO (62%)
285.4	0.2405	H-2→LUMO (26%), H-1→L+1 (33%), HOMO→L+1 (10%), HOMO→L+3 (14%)
279.1	0.3073	HOMO→L+1 (76%)
269.2	0.0202	H-2→LUMO (65%), H-1→L+1 (13%)
254.2	0.0119	H-2→L+2 (19%), HOMO→L+2 (40%)
250.1	0.0181	H-4→LUMO (45%), H-3→LUMO (12%)
242.2	0.0659	H-5→LUMO (50%), H-1→L+1 (12%), HOMO→L+3 (11%)
235.6	0.4185	H-5→LUMO (12%), H-4→LUMO (12%), H-2→L+1 (11%), H-1→L+1 (17%), HOMO→L+3 (28%)
228.0	0.0479	H-5→L+2 (13%), H-3→L+2 (28%), H-1→L+2 (14%)
226.4	0.7095	H-1→L+3 (45%)
223.3	0.0974	H-2→L+1 (11%), HOMO→L+4 (13%), HOMO→L+5 (11%)
216.2	0.0403	H-2→L+1 (29%), HOMO→L+5 (13%)
215.7	0.1164	H-2→L+1 (21%), HOMO→L+6 (20%)
210.9	0.102	H-6→LUMO (36%), HOMO→L+4 (16%), HOMO→L+5 (12%)
210.1	0.0442	H-7→LUMO (15%), H-6→LUMO (11%), HOMO→L+4 (12%), HOMO→L+5 (24%)
209.5	0.019	H-7→LUMO (12%), H-3→L+1 (21%), HOMO→L+6 (10%)
208.7	0.0063	H-7→LUMO (33%), H-3→L+1 (23%)
205.9	0.0358	H-1→L+2 (17%), H-1→L+4 (11%)

Table S-7 Summary of vertical electronic transition properties of **6** computed at the TD-CAM-B3LYP/6-311+G(d,p) level of theory

Wavelength (nm)	***f***	**MO Contributions**
339.8	0.3977	HOMO→LUMO (87%)
314.3	0.058	H-1→LUMO (47%), HOMO→L+1 (38%)
279.3	0.1269	H-2→LUMO (11%), HOMO→L+1 (26%), HOMO→L+2 (52%)
265.3	0.2693	H-2→LUMO (29%), H-1→LUMO (38%), HOMO→L+1 (24%)
254.7	0.2393	H-2→LUMO (51%), HOMO→L+2 (23%)
241.7	0.3014	H-1→L+1 (56%), HOMO→L+4 (17%)
230.1	0.0003	H-4→LUMO (59%), H-4→L+1 (12%), H-4→L+2 (15%)
226.7	0.2459	H-1→L+1 (19%), HOMO→L+4 (56%)
223.9	0.0059	HOMO→L+3 (73%)
221.7	0.4278	H-2→L+1 (10%), H-1→L+2 (59%)
216.7	0.1791	H-3→LUMO (75%)
213.2	0.0584	H-2→L+1 (31%), H-1→L+4 (19%), HOMO→L+4 (12%)
206.4	0.2326	H-2→L+1 (12%), H-2→L+2 (41%)
205.6	0.0076	HOMO→L+5 (28%), HOMO→L+6 (47%)
202.0	0.0011	HOMO→L+5 (39%), HOMO→L+6 (38%)
201.5	0.01	H-3→L+1 (13%), H-2→L+1 (18%), H-2→L+2 (12%), H-1→L+2 (14%), HOMO→L+11 (21%)
192.3	0.0107	H-1→L+3 (57%)
192.0	0.0692	H-5→LUMO (16%), H-3→L+1 (10%), H-1→L+3 (10%), HOMO→L+11 (34%)
190.1	0.0247	HOMO→L+9 (73%)
189.7	0.3996	H-3→L+1 (12%), H-2→L+2 (20%), H-1→L+4 (37%), HOMO→L+11(11%)

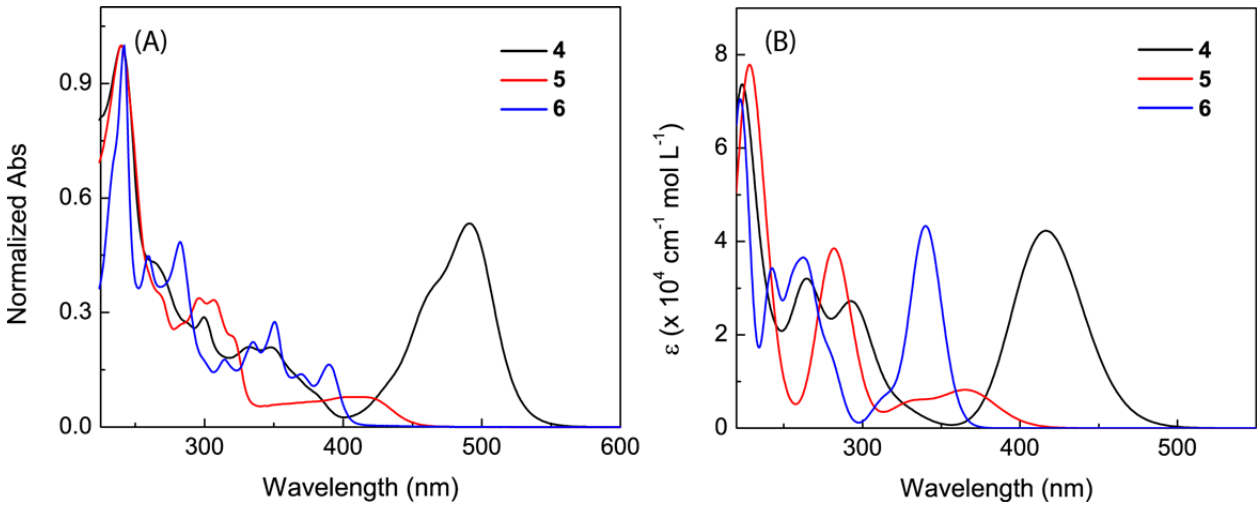

Fig. S-7 Comparison of (A) experimental and (B) TD-DFT calculated UV-Vis spectra for **4-6**.

Table S-8 Summary of experimental UV-Vis absorption data for **4-6**

Entry	UV-Vis absorption λ_{max} / nm (ε / mol^{-1} L cm^{-1})	E_{opt} (eV)
4	488 (3.64×10^3), 346 (1.31×10^3), 329 (sh, 1.38×10^3), 297 (1.85×10^3), 237 (6.75×10^3)	2.35
5	418 (sh, 5.11×10^2), 320 (1.46×10^3), 307 (2.08×10^3), 296 (2.09×10^3), 239 (6.36×10^3)	2.75
6	389 (7.98×10^2), 370 (6.74×10^2), 350 (1.37×10^3), 334, (1.11×10^3), 313(8.63×10^2), 282 (2.39×10^3), 258 (2.21×10^3), 241 (5.00×10^3)	3.07

5. Molecular Orbital Properties of 4-6

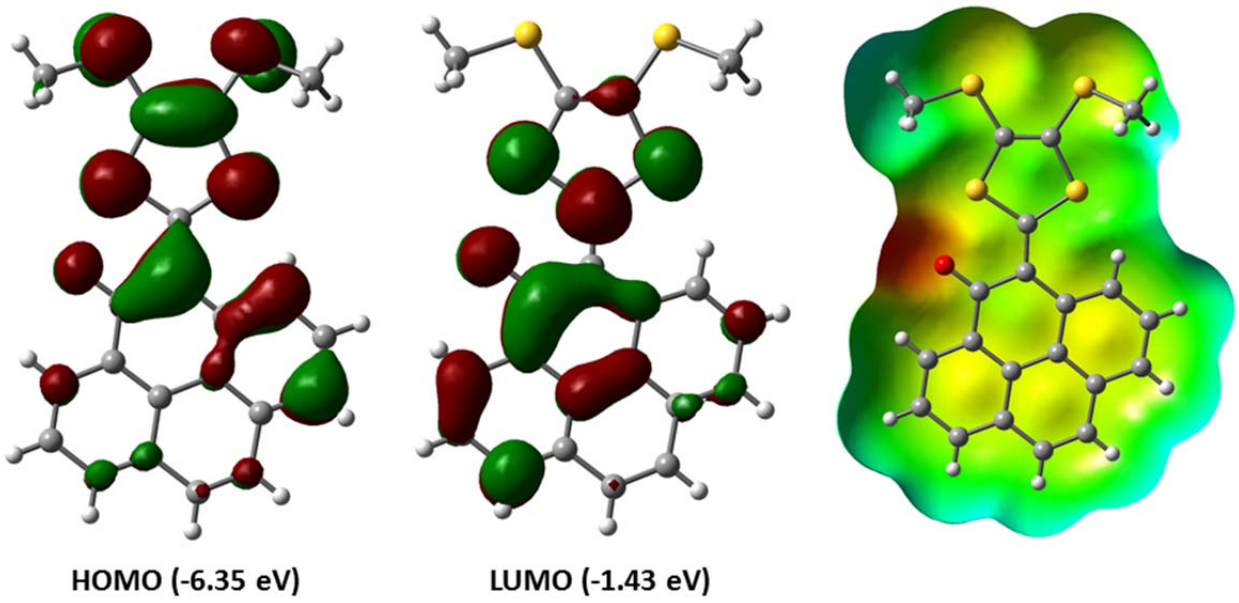

Fig. S-8 Plots of frontier molecular orbitals and electrostatic potential map of **4** calculated at the M06-2X/Def2-SVP level.

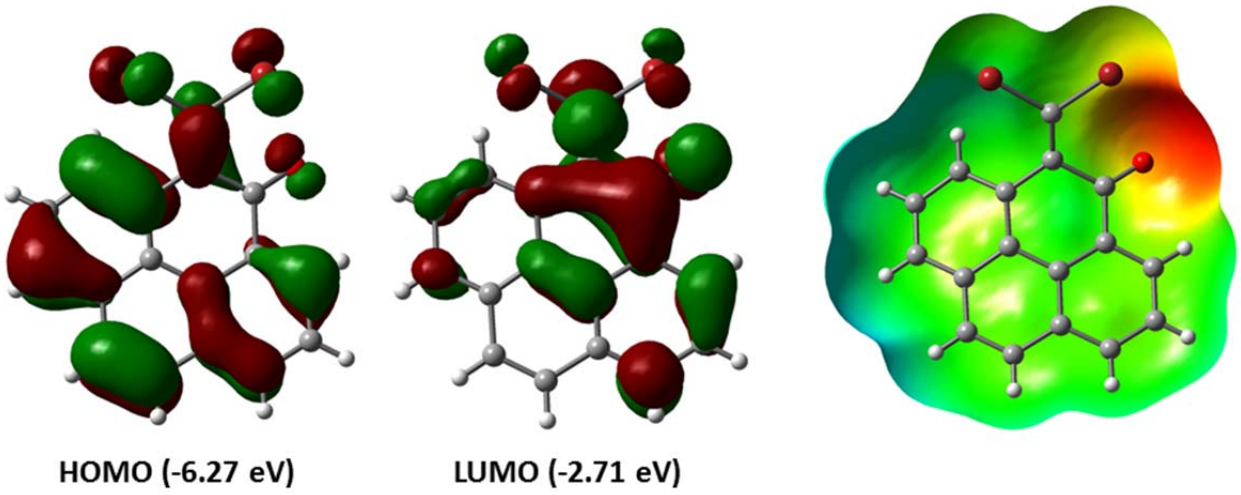

Fig. S-9 Plots of frontier molecular orbitals and electrostatic potential map of **5** calculated at the M06-2X/Def2-SVP level.

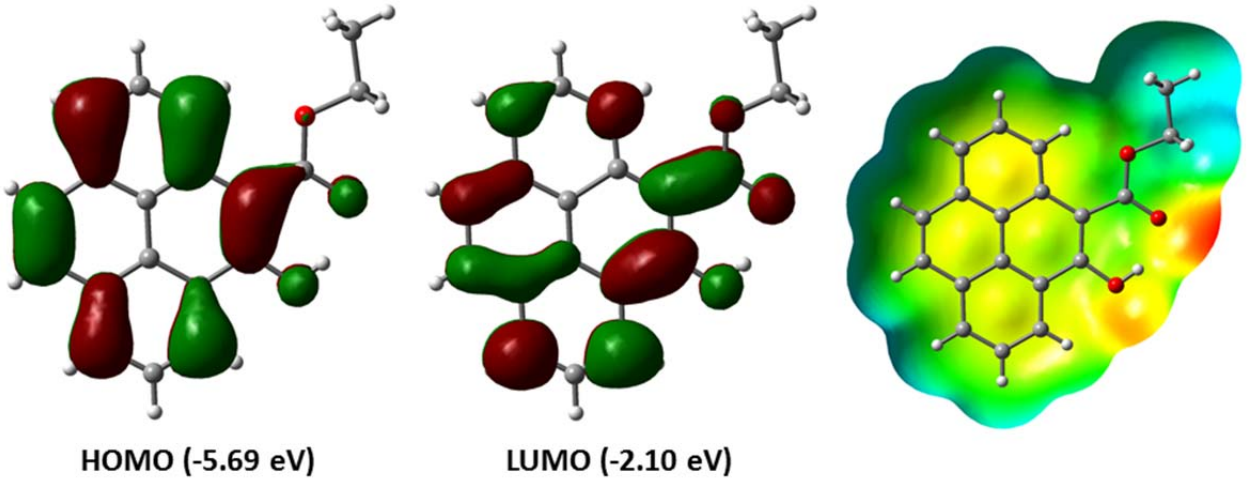

Fig. S-10 Plots of frontier molecular orbitals and electrostatic potential map of **6** calculated at the M06-2X/Def2-SVP level.

6. Results of QTAIM Analysis of 4-6

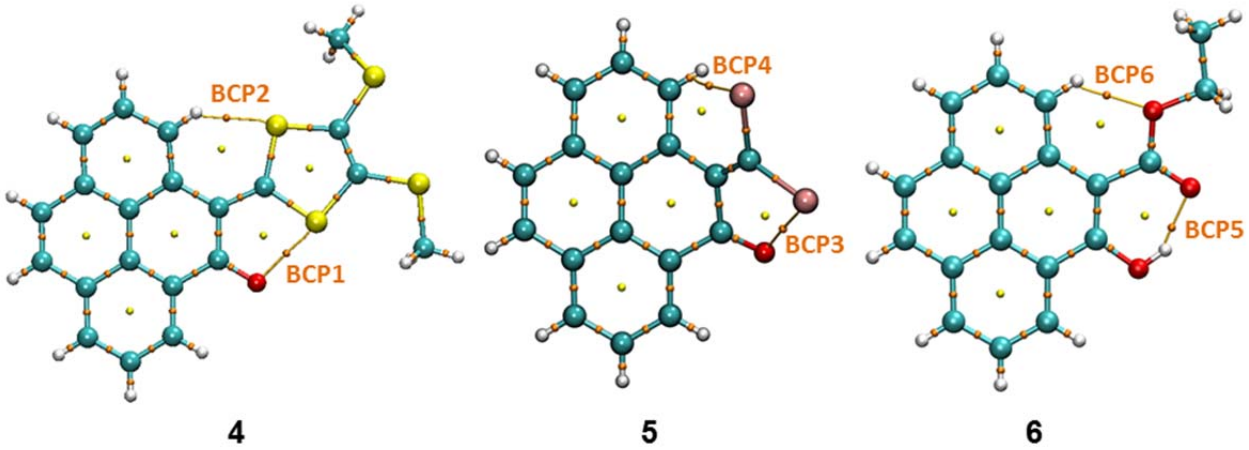

	Type	ρ (a.u.)	$\nabla^2\rho$ (a.u.)	H(r) (a.u.)	ELF	ε
BCP1	(3,-1)	0.0418	0.146	0.001495	0.145	0.150
BCP2	(3,-1)	0.0215	0.0716	0.00120	0.0760	0.0948
BCP3	(3,-1)	0.0165	0.0528	0.000791	0.0580	0.119
BCP4	(3,-1)	0.0129	0.0502	0.002229	0.0375	1.072
BCP5	(3,-1)	0.0444	0.188	0.00238	0.113	0.0187
BCP6	(3,-1)	0.0213	0.0871	0.00190	0.0529	0.0342

Fig. S-11 Molecular topological graphs obtained from QTAIM analysis for compound **4** computed at M06-2X/Def2-SVP level of theory.

7. Fluorescence Spectral Data for Compound 6

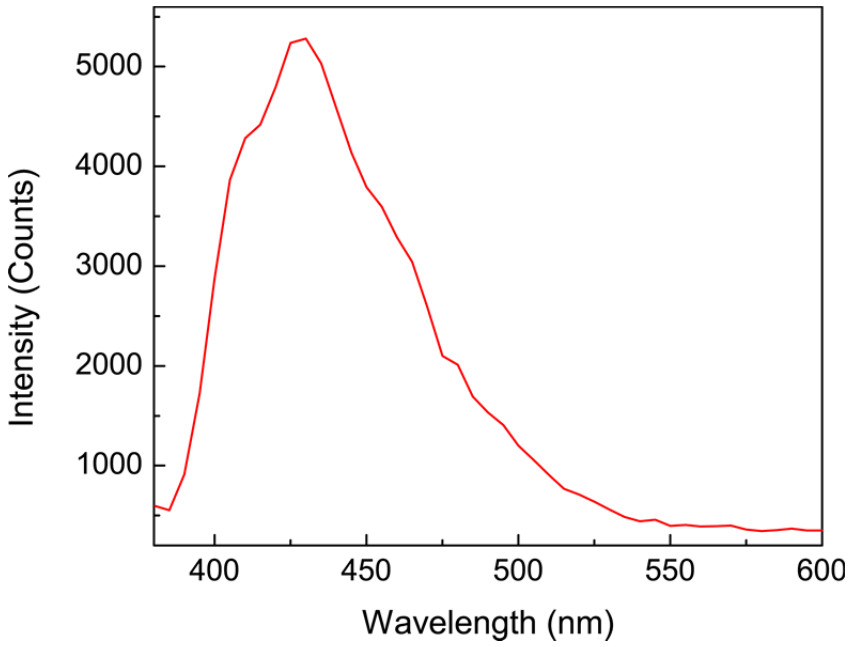

Fig. S-12 Fluorescence spectrum of compound **6** (1.56×10^{-5} M) measured in CH_2Cl_2 at room temperature. Relative quantum yield (Φ) is 7.6% (using quinine sulfate, Φ = 54.6%, as the standard).